Simulation Methodology for Pressure Tube Integrity Analysis and Comparison with Experiments

G.H. Archinoff, J.C. Luxat, P.D. Lowe, K.E. Locke, and A.P. Muzumdar
Ontario Hydro
Nuclear Studies and Safety Department
700 University Avenue
Toronto, Ontario
M5G 1X6

Abstract
The computer code SMARTT (Simulation Method for Azimuthal and Radial Temperature Transients) is used in safety analysis of Ontario Hydro's CANDU reactors to predict fuel and pressure tube thermal and mechanical behaviour under asymmetric coolant conditions, such as stratified flow. This paper presents comparisons of SMARTT predictions, with preliminary results of two experiments in which large temperature non-uniformities developed on pressure tubes undergoing heatup and transverse strain at 1.0 MPa internal pressure. Temperature asymmetries developed as a result of slow boil-off of coolant in the channel. The SMARTT temperature predictions are shown to agree well with the experimental results. SMARTT accurately predicts the time at which the pressure tube balloons into contact with the calandria tube. The transient liquid level in the channel can also be accurately predicted using a simple venting / boil-off model.

Résumé
Le code de calcul SMARTT (Simulated Method for Azimuthal and Radial Temperature Transients – méthode de simulation pour les variations de température azimutale et radiale) est utilisé dans l'analyse de la sûreté des réacteurs CANDU d'Ontario Hydro pour prédire le comportement mécanique et thermique des tubes de force et des crayons de combustible soumis à des conditions assymétriques du caloporteur, comme dans le cas d'un régime stratifié. Ce document compare les résultats obtenus avec le code SMARTT avec les résultats préliminaires de deux expériences ayant enregistré des écarts importants de température sur les tubes de force causés par l'ébullition lente du caloporteur dans le canal de combustible et une tension transversale causée par une pression interne de 1 MPa. Les températures calculées par le code SMARTT sont en bon accord avec les résultats expérimentaux. Le code SMARTT calcule avec exactitude le moment où le tube de force flue et entre en contact avec le tube de calandre. Il est également possible de calculer avec précision le niveau de liquide dans le canal en utilisant un modèle simple d'éventage / ébullition.

Introduction
One of the objectives of safety analysis of CANDU reactors is to demonstrate that a postulated accident does not lead to rupture of the fuel channels. The computer code SMARTT (Simulation Method for Azimuthal and Radial Temperature Transients) [1] is one of the analytical tools used in the analysis of fuel channel integrity. SMARTT models fuel and pressure tube thermal behaviour under asymmetric fuel cooling conditions, such as stratified coolant flow. Such conditions can lead to non-uniform pressure tube heatup in the circumferential direction. If there is a highly localized hot region on the pressure tube circumference while the pressure tube is undergoing transverse strain (ballooning), the pressure tube may fail prior to contacting its calandria tube. SMARTT predicts the pressure tube circumferential temperature distribution and its associated effects on pressure tube ballooning, and whether the pressure tube will fail, or whether it will contact the calandria tube.

This paper describes comparisons between SMARTT predictions and preliminary results of two experiments in which pressure tubes were heated up to initiate ballooning under the influence of non-uniform circumferential temperature distributions. The temperature non-uniformities arose as a result of slow boil-off of coolant in the channel. The pressure tube ballooned into contact with the calandria tube, without failure, in both experiments.

The experimental apparatus and results are described first, followed by a discussion of the modification implemented in SMARTT in order to simulate the experiments. The treatment of the thermal-hydraulic boundary conditions required as input data to SMARTT is then

Keywords: nuclear safety, pressure tubes, LOCA.

described. SMARTT predictions are presented and compared to the experimental results. Areas of disagreement and agreement are discussed, along with their implications for the validity of the models used in the simulations.

Description of Experimental Apparatus and Results

A series of four pressure tube circumferential temperature distribution experiments is being performed under CANDEV at Whiteshell Nuclear Research Establishment. Two of these experiments have been completed [2]. Preliminary results from these two tests are described below. A detailed description of the experiments and analysis of the results will be available when the series of experiments is completed.

The apparatus consisted of a 2.3-metre-long segment of a CANDU-type fuel channel, as shown in Figure 1. The pressure tube was closed at one end and open to a vertical pipe (1.16 cm ID) at the other. In the channel, 36 indirect heaters were grouped into three different rings. These heaters, together with a supporting central tube, formed the CANDU-type 37-element fuel bundle configuration. The power distribution to the three rings of heaters is shown in Figure 2.

Thermocouples were placed on the outside of the pressure tube to monitor its temperature distribution during the experiments. Their locations were different in the two tests (see Figure 1). In the second test, thermocouples were also placed on the heater sheaths. The temperature of the fluid at the exit of the channel was also measured. The vertical pipe was connected to a surge tank so that the pressure in the channel could be kept relatively constant at 1 MPa during the experiment. The channel was immersed in a pool of water (23°C at 1 atmosphere) to simulate the moderator.

At the start of each test, the water in the pressure tube was heated slowly from room temperature. When the thermocouples on the top of the pressure tube registered saturation temperature (181°C), the power to the heaters was raised to a preset level, as shown in Figure 2. The experiment terminated when the heaters failed. In both tests the pressure tube was dry fully around its circumference when this happened.

Figure 3 shows an example of the circumferential temperature distribution measured around the outside of the pressure tube. Just before the power was raised, the temperature distribution varied from saturation at the top to subcooled at the bottom. The water inside the pressure tube should have had a similar distribution, as the heat transfer across the pressure tube was low. As the power was increased, water boiled off gradually. The inside of the pressure tube became

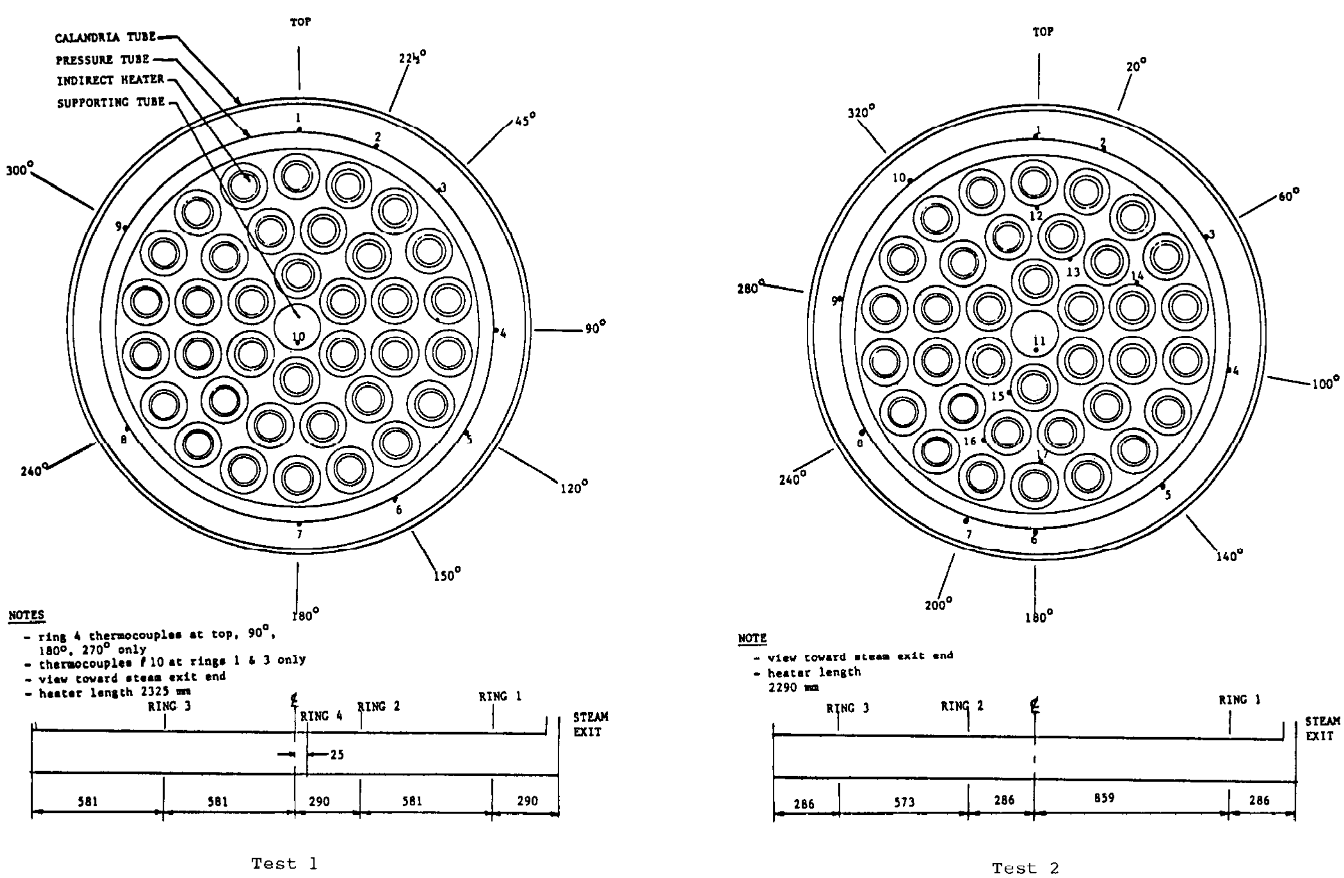

Figure 1: Schematic of the pressure tube circumferential temperature distribution experiment.

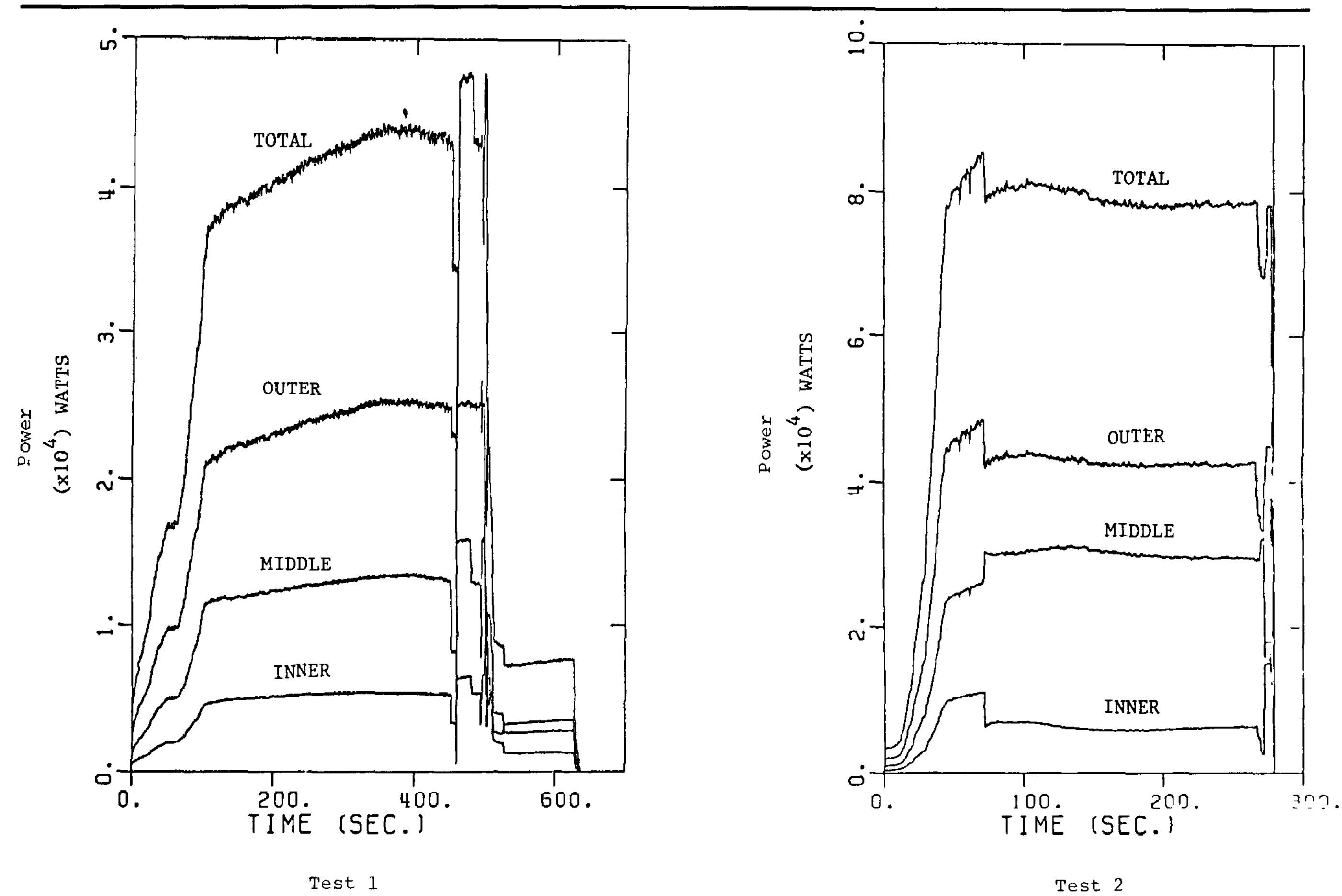

Figure 2: Power input to the indirect heaters.

exposed to steam, in succession from top to bottom. This is reflected by the sequence of sudden rises in temperature above saturation on the thermocouple readings in Figure 3. The pressure tube strained as the temperature increased. When the pressure tube came into contact with the calandria tube, heat transfer to the moderator water increased, which caused a decrease in the pressure tube temperature. The decrease in pressure tube temperature was limited by an apparently low contact conductance between the pressure tube and calandria tube. This low contact conductance was likely a result of interference by thermocouple cables located between the two tubes.

The axial temperature gradients were relatively small when compared to the circumferential temperature gradients. In general, the axial temperature distribution had a maximum in the middle of the channel.

SMARTT Model

The 37-element SMARTT model is described in detail in Reference 1. Although the geometry of the experimental rig is identical to that of a segment of a fuel channel containing a 37-element bundle, the fuel element simulator internal geometry and materials are different from those of a CANDU fuel bundle. Each simulator consists of a pressurized water reactor (PWR) fuel sheath, contained concentrically within a Bruce-size CANDU sheath (as shown in Figure 1). Helium gas fills the internal voids. Power is applied directly to the PWR sheath, which heats the CANDU sheath *via* radiation and conduction through the helium. SMARTT was modified to model this heater geometry.

Figure 4 shows the SMARTT model of a standard CANDU fuel element, and the SMARTT model of the fuel element simulators used in the experiments. The fuel element simulator is modelled exactly, with the two innermost radial nodes treated as helium. The third and fourth nodes are Zircaloy, representing the PWR sheath heater. The fifth node is helium, and the sixth node is Zircaloy, representing the CANDU fuel sheath. This was the only modification made to the models in SMARTT for the simulation of the experiments.

Boundary Conditions

The important input data required by SMARTT are the power transient, the pressure transient, the coolant temperature transient in each subchannel, and the transient convective heat transfer coefficient on each sheath and pressure tube surface node. This information was obtained either directly from experimental

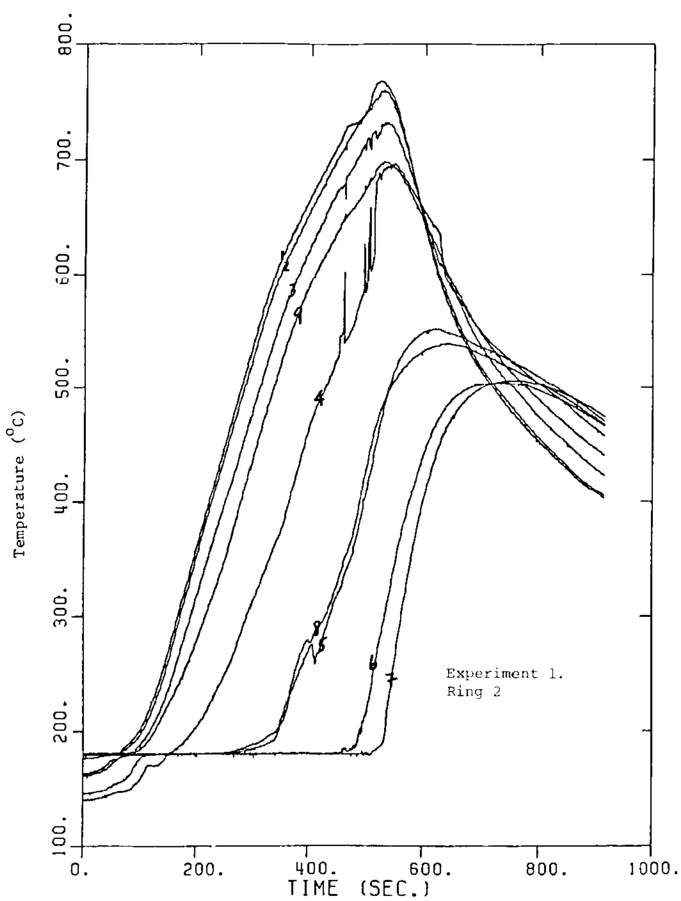

Figure 3: Measured pressure tube circumferential temperature distribution.

measurements (power and pressure), or was derived using simple models or approximations (thermal-hydraulic boundary conditions).

The power and pressure transients were obtained directly from measured values. The pressure in both tests was approximately constant at 1.0 MPa. The power in the first test was about 40 kW, which corresponds to about 1% of full power for a 7.5 MW channel. The power in the second test was 80 kW.

For simplicity in modelling, two types of thermal-hydraulic subchannels are defined. The first type is characterized by good convective heat transfer to saturated liquid. The heat transfer coefficient is assumed to be 50 kW / m^{2}K, a value which is sufficient to provide an adequate heat sink for the power generated in the fuel. This type of subchannel represents portions of the bundle covered by liquid and cooled by boiling heat transfer. The second type of subchannel represents portions of the bundle exposed to steam only, and is characterized by significantly lower convective heat transfer to steam.

The convective heat transfer coefficient for the steam filled subchannels is derived from

$$Nu = \frac{hd}{k} = 4 \qquad (1)$$

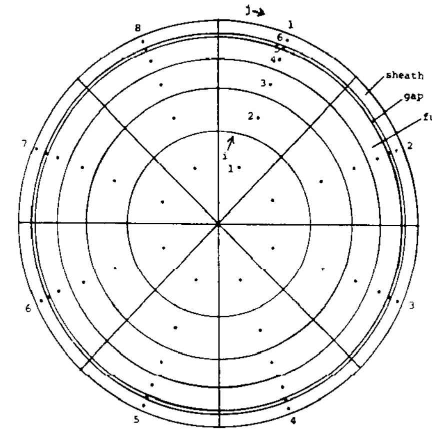

Nodalization for Standard Bruce-type Fuel Element

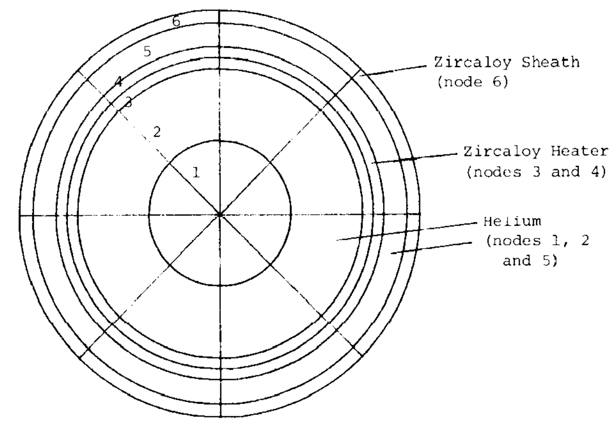

Nodalization for Experimental Heater Fuel Element

Figure 4: SMARTT fuel element nodalization.

where

Nu = Nusselt number
d = hydraulic diameter
k = thermal conductivity of steam
h = heat transfer coefficient.

A Nusselt number equal to 4 approximates laminar cooling. This was judged to be a reasonable assumption, since the mass flow rate of steam at the centre of the channel is estimated to be typically less than 10 g / s, based on the observed boil-off rate. This results in Reynolds numbers within the laminar regime.

Coolant temperatures in the steam-filled subchannels are estimated by setting them equal to the average of the temperatures of the sheath surfaces encompassing each subchannel, weighted by the arc length of each surface. This approximation is also consistent with low flowrates of steam, and implies that steam cooling or heating is not a dominant factor in these experiments. This approach permits heat transfer in the vertical direction, since lower fuel elements may be

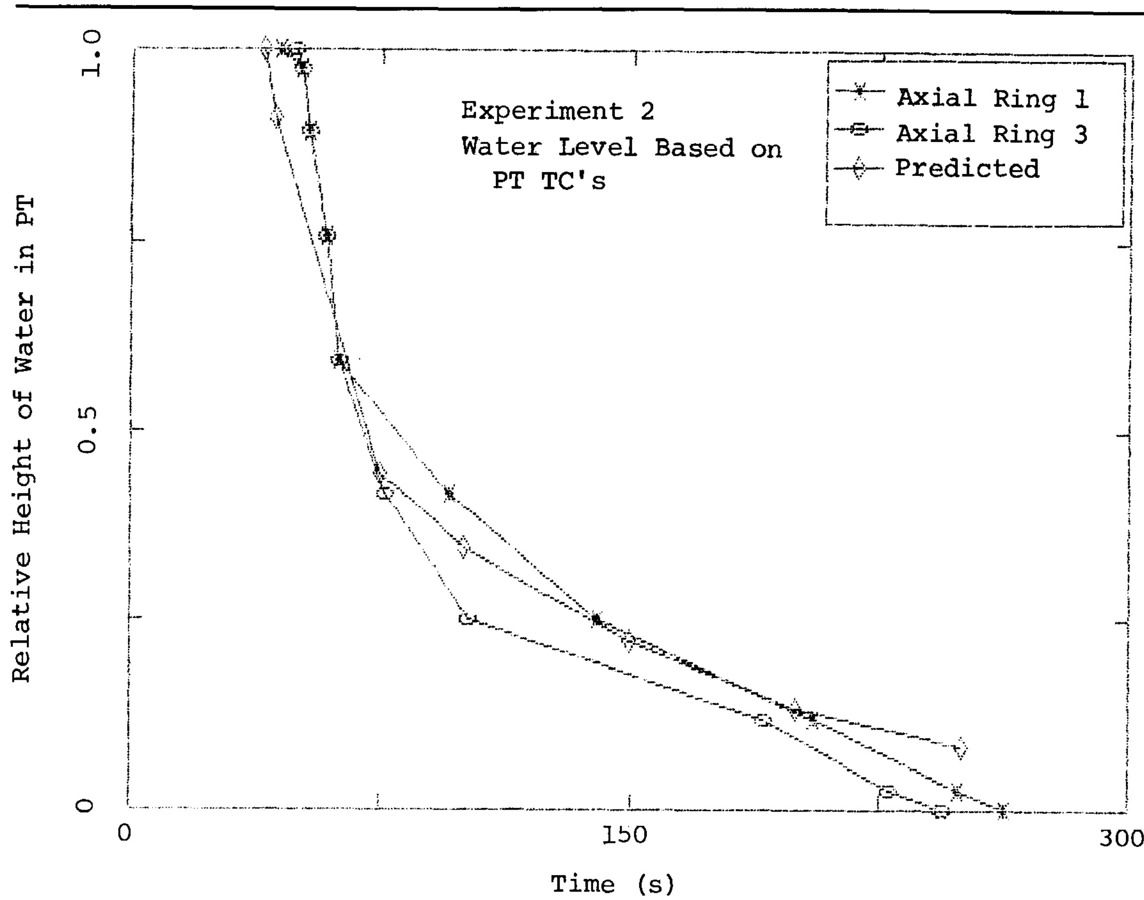

Figure 5: Predicted and inferred water level transients in test 2.

covered by liquid while upper elements are exposed to steam. Heat transfer from hot, upper elements in a subchannel to the steam in the subchannel, and then to the cooler lower elements, simulates the actual effect of the liquid heat sink at the bottom of the channel.

The timing of the transition from water-filled to steam-filled in any subchannel is derived using the venting / boil-off model described in Reference 3. This model predicts the average steam fill fraction in the channel using the measured power transient and the hydraulic resistances associated with the experimental rig. Minor modifications were made to the model to account for venting from the test section with one end closed.

In the experiments, the vertical portion of the piping between the channel exit and the condenser is initially liquid filled. Steam generated in the channel must overcome the static head of the liquid in the exit piping prior to venting from the channel. Subsequently, the rate of venting from the channel depends on the pressure difference between the channel and the condenser, the steam generation rate, and the hydraulic losses in the exit piping. When the liquid level drops to the point where the steam generation rate is not sufficient to maintain an excess pressure in the channel, the subsequent liquid level transient is governed by simple boil-off. The venting / boil-off model accounts for these processes, and predicts an average liquid level transient.

This information is used in SMARTT by defining subchannels above the calculated liquid level to be steam filled, and the subchannels below the calculated liquid level to be liquid filled. SMARTT considers seven possible liquid levels, ranging from a liquid-filled channel to a steam-filled channel. The timing of the transition from one level to the next is based on the level transient derived using the venting / boil-off model.

Comparison with Experiments

The second experiment was conducted with thermocouples monitoring fuel sheath temperatures as well as pressure tube temperatures, whereas in the first test only pressure tube thermocouples were used. Because of this, and because some heater elements burned out prior to the pressure tube reaching temperatures at which it would balloon in the first test, the emphasis of the comparison of predictions with measurements is on the second test.

Figure 5 compares the predicted average water level transient with the transient inferred from measurements of pressure tube thermocouples in Test 2. The inferred transient is derived by assuming that the tim-

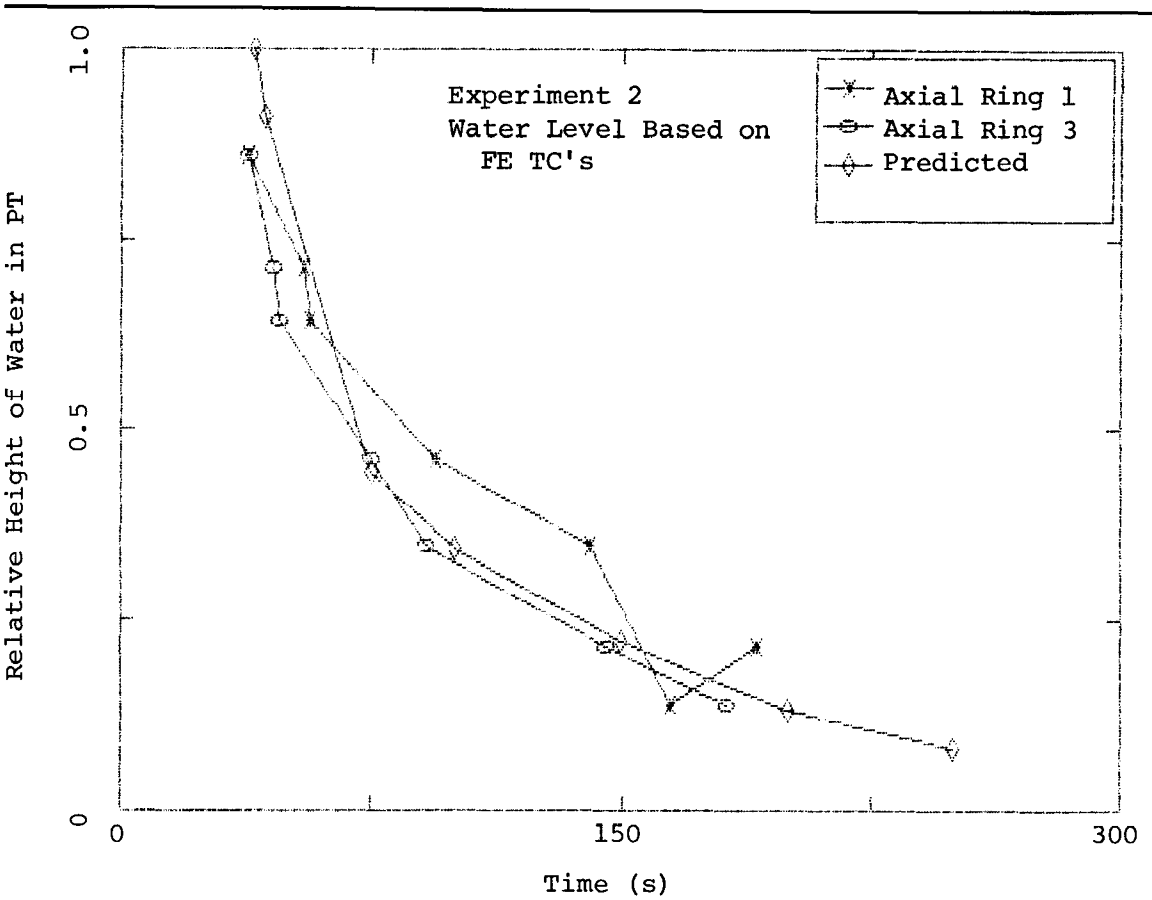

Figure 6: Predicted and inferred water level transients in test 2.

ing of the first indication of dryout on a thermocouple is the time the water level reaches the height of that thermocouple. Thus, two inferred water level transients are shown in Figure 5, one derived from the set of pressure tube thermocouples in Ring 1 in Figure 1, the other based on thermocouples in Ring 3. Similarly, Figure 6 compares the predicted water level transient with transients inferred from fuel element thermocouples in Rings 1 and 3, respectively.

Figures 5 and 6 show that the predictions of the simple venting / boil-off model are in good agreement with water level transients inferred from thermocouple measurements. In particular, the initial rapid drop in level, corresponding to venting from the channel, is very well predicted. The figures also show that, according to the thermocouple indications, the fuel elements in the upper portion of the channel experience dryout before the pressure tube, while the converse is true in the bottom portion of the channel.

Figure 7 compares SMARTT predictions with measurements of temperature at the top of the pressure tube (thermocouple 1 in Rings 1, 2, and 3 in Figure 1). SMARTT slightly underpredicts the temperatures initially, however the agreement towards the end of the transient is excellent. (The comparisons are terminated at the time of predicted pressure tube ballooning contact with the calandria tube, which, as discussed later, is in good agreement with observed time of ballooning contact.)

Figure 8 compares SMARTT predictions of temperatures at the side of the pressure tube (100 degrees from the top) with measurements from thermocouple 4 in Rings 1, 2, and 3 (see Figure 1). The SMARTT predictions fall within the range of the experimentally observed temperatures.

Figure 9 compares the pressure tube circumferential temperature profile predicted by SMARTT at 225 seconds (10 seconds prior to ballooning contact), with the experimentally observed profile at the same time at axial Rings 1, 2, and 3. Again, the SMARTT predictions are in good agreement with the experimental observations, falling within the range of measured temperatures.

Figures 10 and 11 compare the SMARTT predictions of fuel sheath temperature with results obtained from thermocouples 12 and 14 in Rings 1 and 3. These thermocouples are located on the underside of the top fuel element in the outer ring of elements, and on the top of the fuel element located at 60 degrees in the intermiediate ring, respectively (see Figure 1). The thermocouple transients are terminated at the times when the readings become irrational, indicating the thermocouples have failed.

Figures 10 and 11 show a significant axial variation in the measured fuel temperature, with the fuel at the

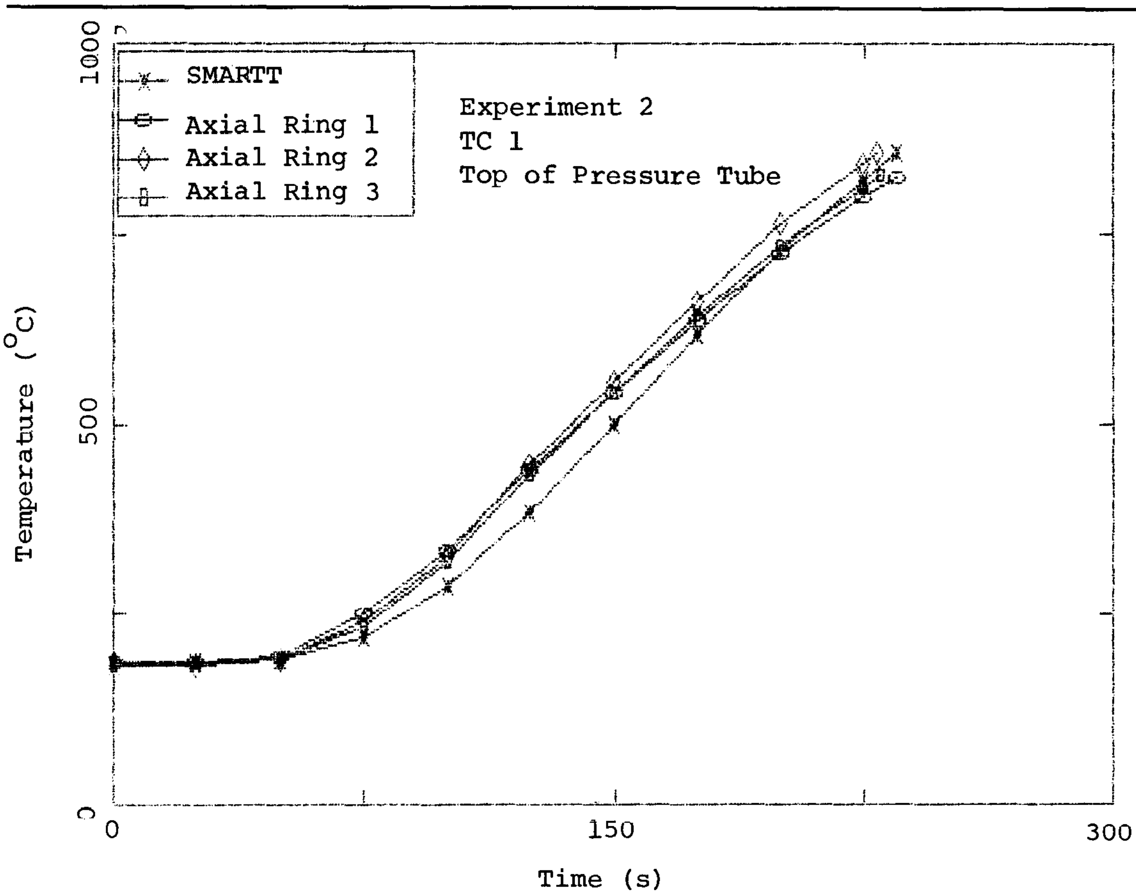

Figure 7: Comparison of measured and predicted temperatures at top of pressure tube in test 2.

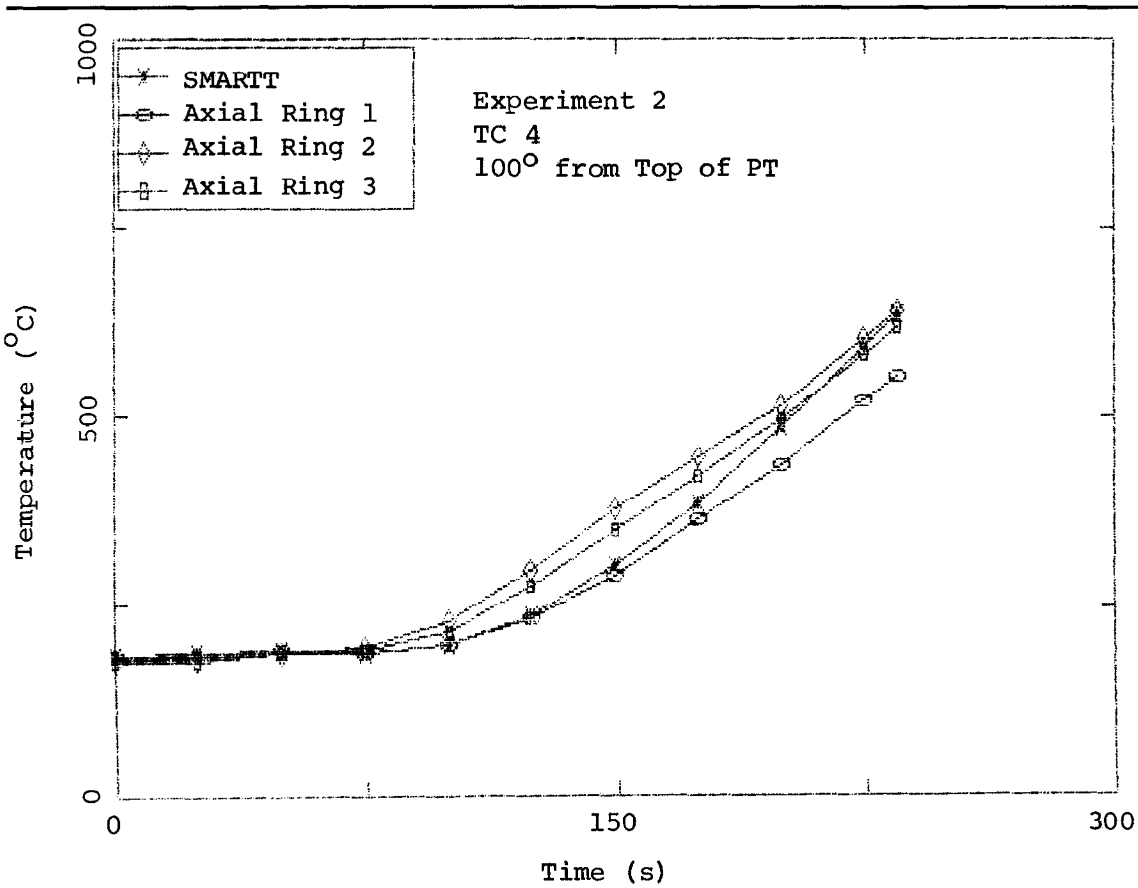

Figure 8: Comparison of measured and predicted temperatures at side of pressure tube in test 2.

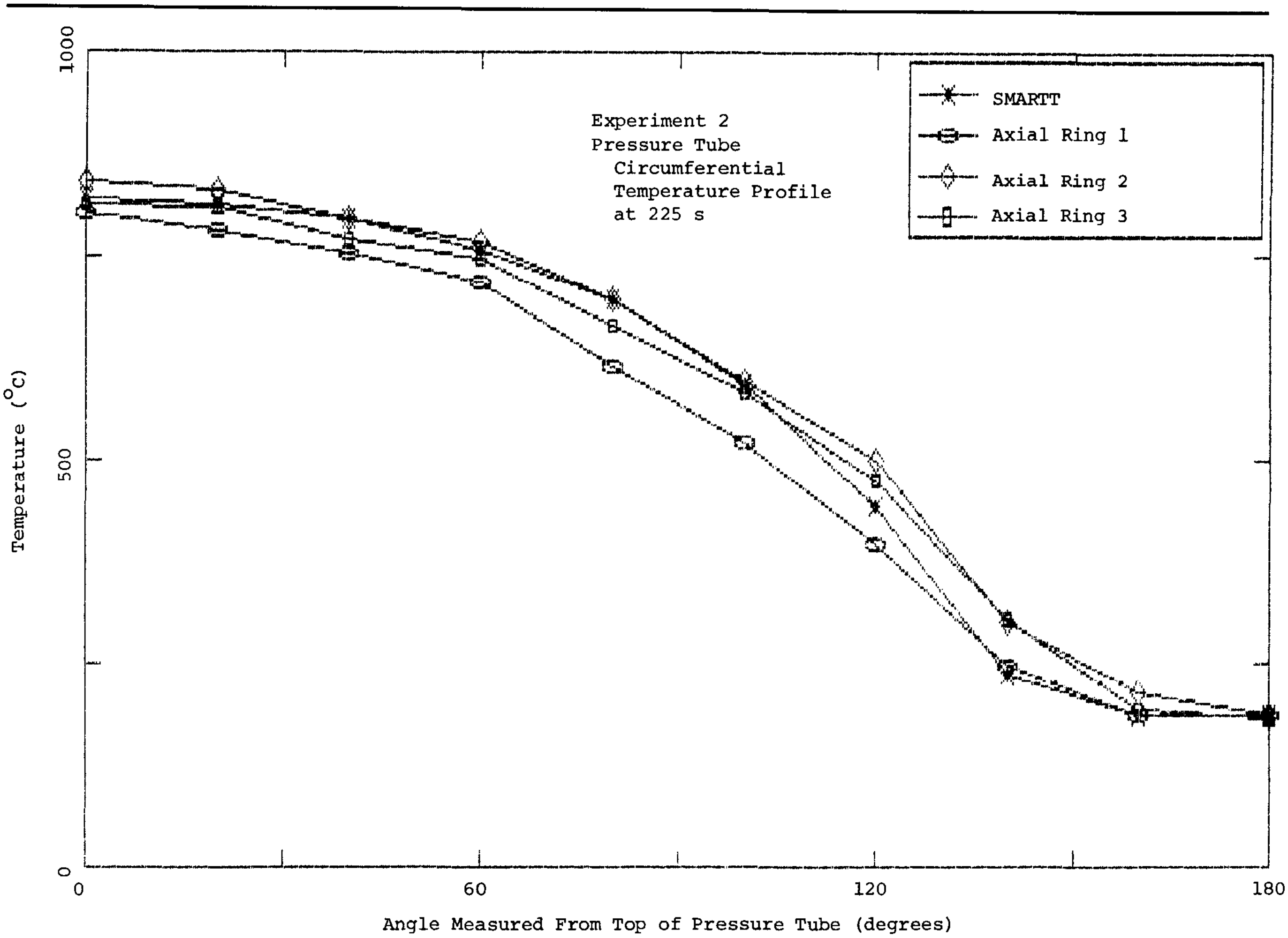

Figure 9: Comparison of measured and predicted pressure tube circumferential temperature profile in test 2.

outlet end exhibiting lower temperatures. The variation ranges from 50–100°C on the top fuel element, to 100–200°C on the intermediate ring element. This axial variation is likely due to convective cooling by steam, which would have a greater effect toward the channel outlet end, as observed. The SMARTT predictions generally fall between the two thermocouple transients on each figure, but are closer to the transients recorded at axial Ring 1.

The final comparisons presented for test 2 are of the observed and predicted times of pressure tube ballooning, and the observed and predicted local pressure tube strains following ballooning. Table 1 compares the time of pressure tube / calandria tube contact predicted by SMARTT with the contact inferred from pressure tube thermocouple measurements (indicated by a sharp decrease in temperature). SMARTT predicts a single time of contact for all points on the pressure tube circumference, because the tube is assumed to remain circular and concentric within the calandria tube. Thus, the pressure tube is assumed to touch the calandria tube at the same time at all locations on its circumference. Based on the pressure tube thermocouple measurements, however, the pressure tube contacts the calandria tube at the top first, followed by a gradual spreading of contact in the circumferential direction. This phenomenon is accentuated at Rings 1 and 3, which are near the closed and outlet ends of the channel, and may be influenced by end effects. Ballooning appears to be more uniform at Ring 2, near the centre of the channel. The SMARTT-predicted contact time is in good agreement with the contact time at the top of the pressure tube at all three axial positions.

Table 2 shows the observed and predicted pressure tube wall thickness at the end of the test. SMARTT overpredicts the degree of wall thinning at the top of the pressure tube. This is consistent with the apparent non-circular ballooning behaviour in the experiment, which would cause the pressure tube to contact the calandria tube with less-than-predicted wall thinning.

Figures 12 and 13 compare predictions of water level and top pressure tube temperature with results of test 1. The initial rapid drop in water level is slightly underpredicted, leading to a slight underprediction of

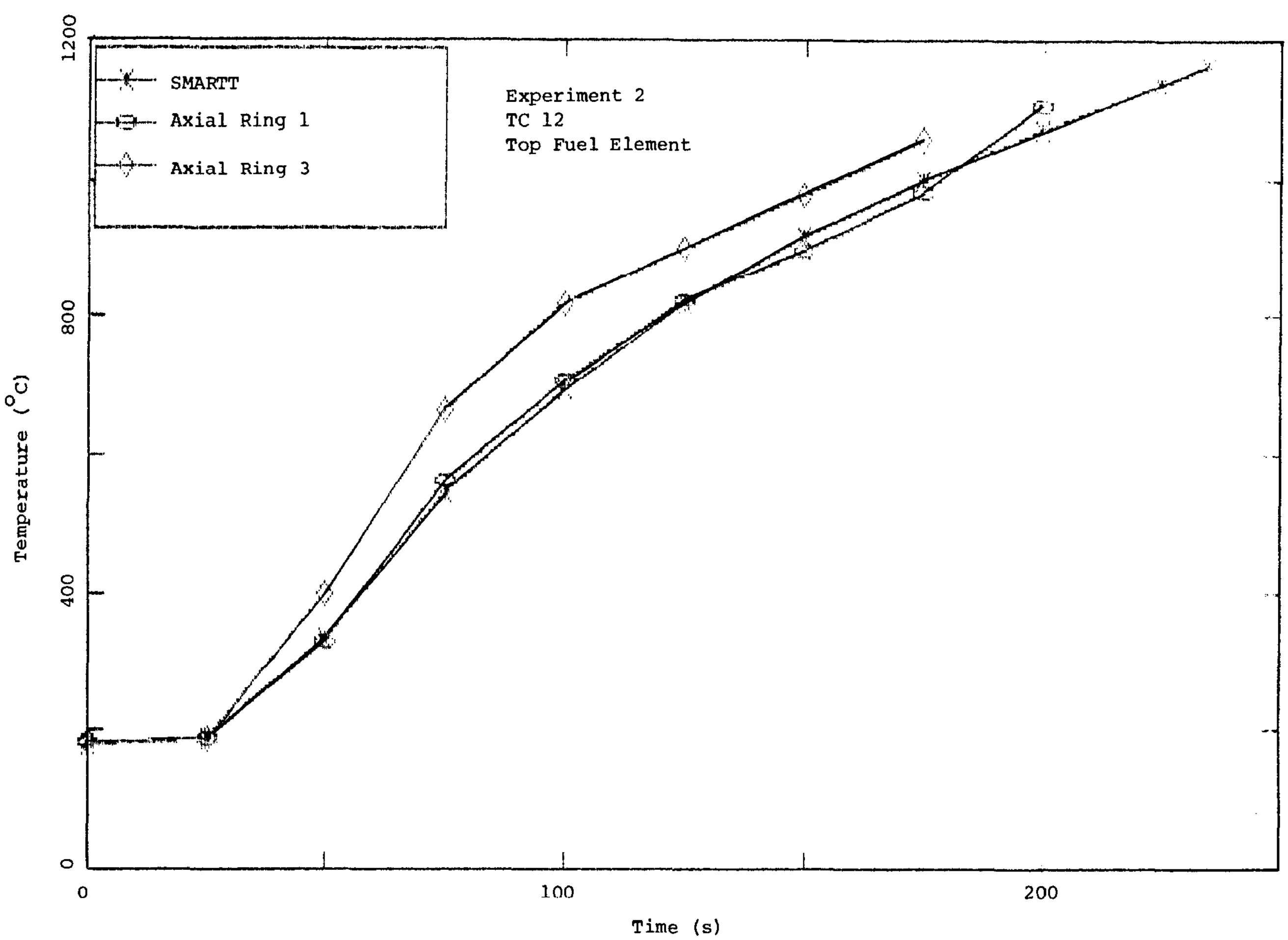

Figure 10: Comparison of measured and predicted fuel sheath temperatures in test 2.

pressure tube temperature in the early part of the transient. Toward the end of the transient, however, the pressure tube temperature is accurately predicted.

Discussion

The comparisons in Figures 5–13 show that the combination of the venting / boil-off model described in Reference 3, and SMARTT, using simple thermal-hydraulic boundary conditions, predicts the outcome of the experiments with good accuracy. Pressure tube temperatures as well as fuel temperatures are well predicted, as is the time of pressure tube / calandria tube contact.

Additional improvements in accuracy can likely be obtained by making further use of the venting / boil-off model. In addition to predicting the transient steam fill fraction used in the simulations described herein, this model also predicts steam temperatures and convective heat transfer coefficients as functions of axial position in the channel. This thermal-hydraulic information can be used in SMARTT instead of the simple assumption described earlier. The model can also be explicitly discretized in the axial direction, allowing the prediction of stem fill fraction to be dependent on axial position. With these refinements the venting / boil-off model – SMARTT combination can be used to predict fuel and pressure tube response at any axial position in the channel.

The comparisons in this paper show that the venting / boil-off model – SMARTT combination can be used with confidence in reactor safety analysis, at least when conditions are similar to those of the experiments. The combination of these two models is sufficient to carry out a complete analysis of pressure tube integrity, since the only required input conditions are the power, header pressures, and initial void and temperature distributions, and this information is typically generated by network thermal-hydraulic codes. The range of validity of the models will be expanded as more experiments in this series are completed.

Conclusions

This paper has presented comparisons of predictions with initial measurements obtained from the first two pressure tube temperature gradient tests performed under CANDEV at WNRE. The comparisons show that

1. the transient steam fill fraction in the channel is well

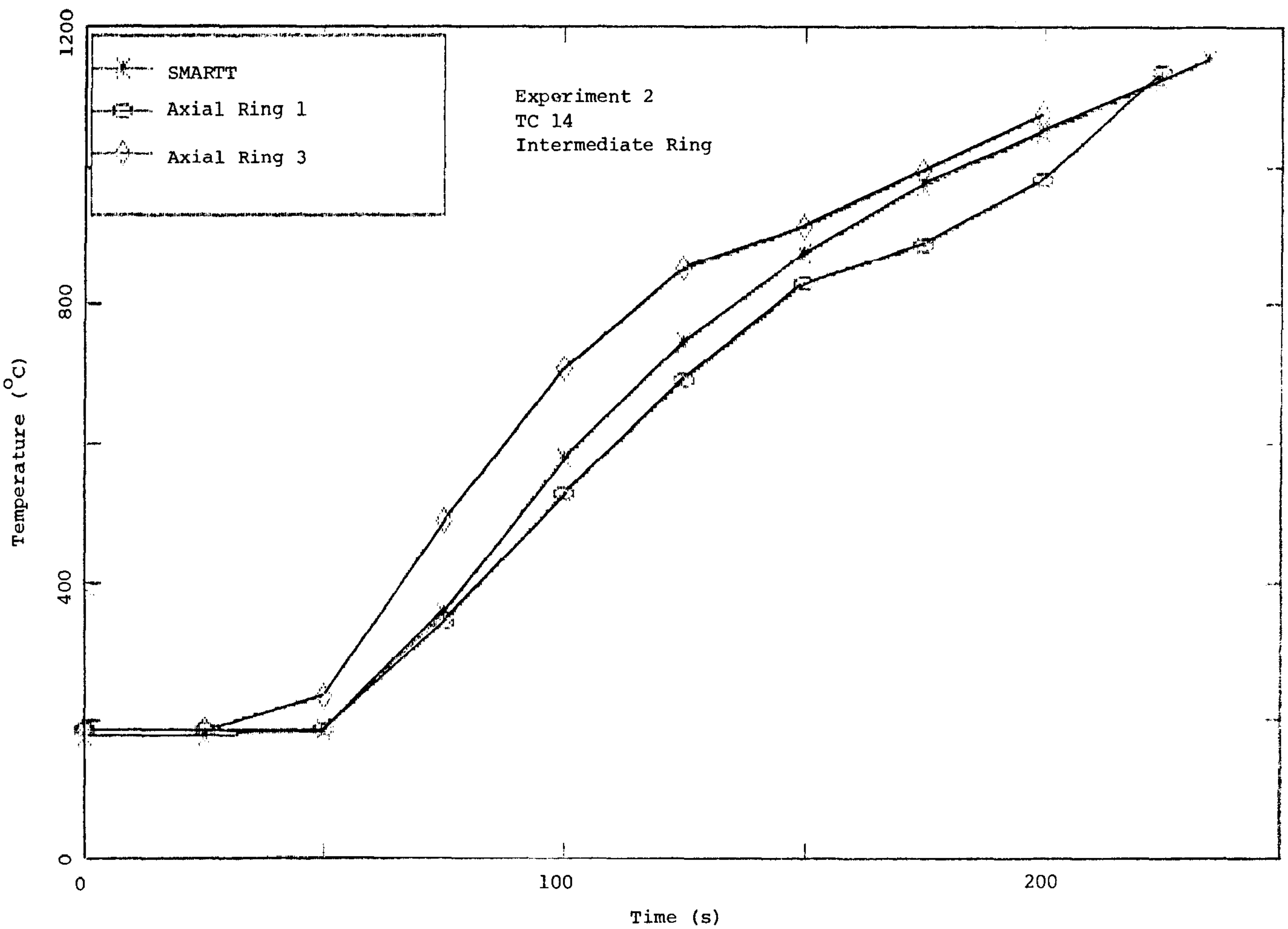

Figure 11: Comparison of measured and predicted fuel sheath temperatures in test 2.

predicted using the venting / boil-off model described in Reference 3;

2. fuel and pressure tube temperatures are accurately predicted by SMARTT when the transient steam fill fraction is obtained from the venting / boil-off model and simple thermal-hydraulic boundary conditions are used;
3. the time of pressure tube / calandria tube contact at the top of the pressure tube is accurately predicted by SMARTT; and

Table 1: Time of PT / CT Contact Test 2

SMARTT prediction	*235 s*		
Circumferential contact position (degrees)	*Ring 1*	*Ring 2*	*Ring 3*
0	241 s	229 s	230 s
20	238	232	238
40	247	235	250
60	254	238	253
80	283	247	263
100	293	254	271

Table 2: Post-Test PT Wall Thickness Test 2

Circumferential angle (degrees)	*Measured thickness (mm)*			*SMARTT prediction (mm)*
	Ring 1	*Ring 2*	*Ring 3*	
0	3.23	3.20	3.33	1.87
top				
20	3.26	3.12	3.18	2.25
60	3.70	3.40	3.48	3.77
100	3.76	4.04	4.01	4.15
180	4.08	4.15	4.15	4.15
bottom				

4. the venting / boil-off model – SMARTT combination can be used for reactor analysis with confidence in the accuracy of the results, when the accident conditions are similar to those of the experiments.

Acknowledgements

The experimental results described in this paper are the property of CANDU Owners Group (COG). No exploitation or transfer of this information is permitted in the absence of an agreement with COG, nor may this

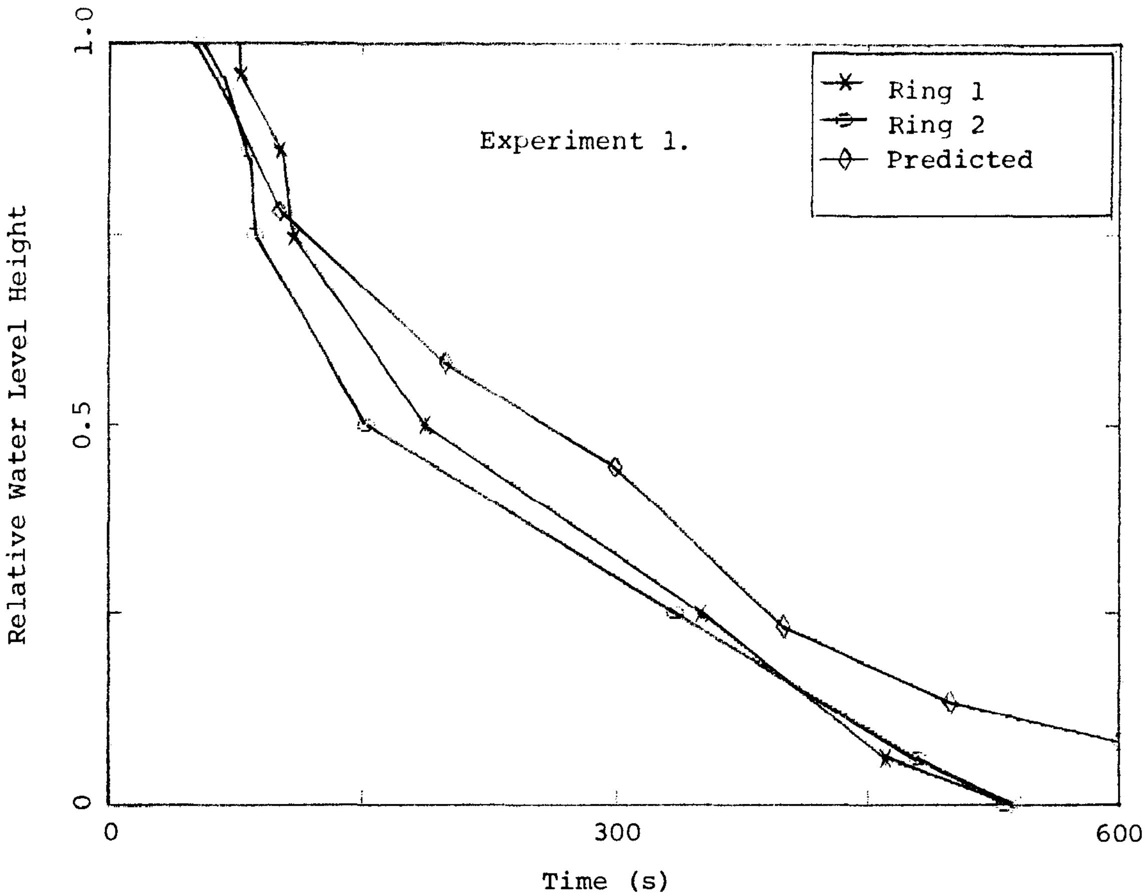

Figure 12: Comparison of predicted water level transient with transient inferred from PT thermocouples in test 1.

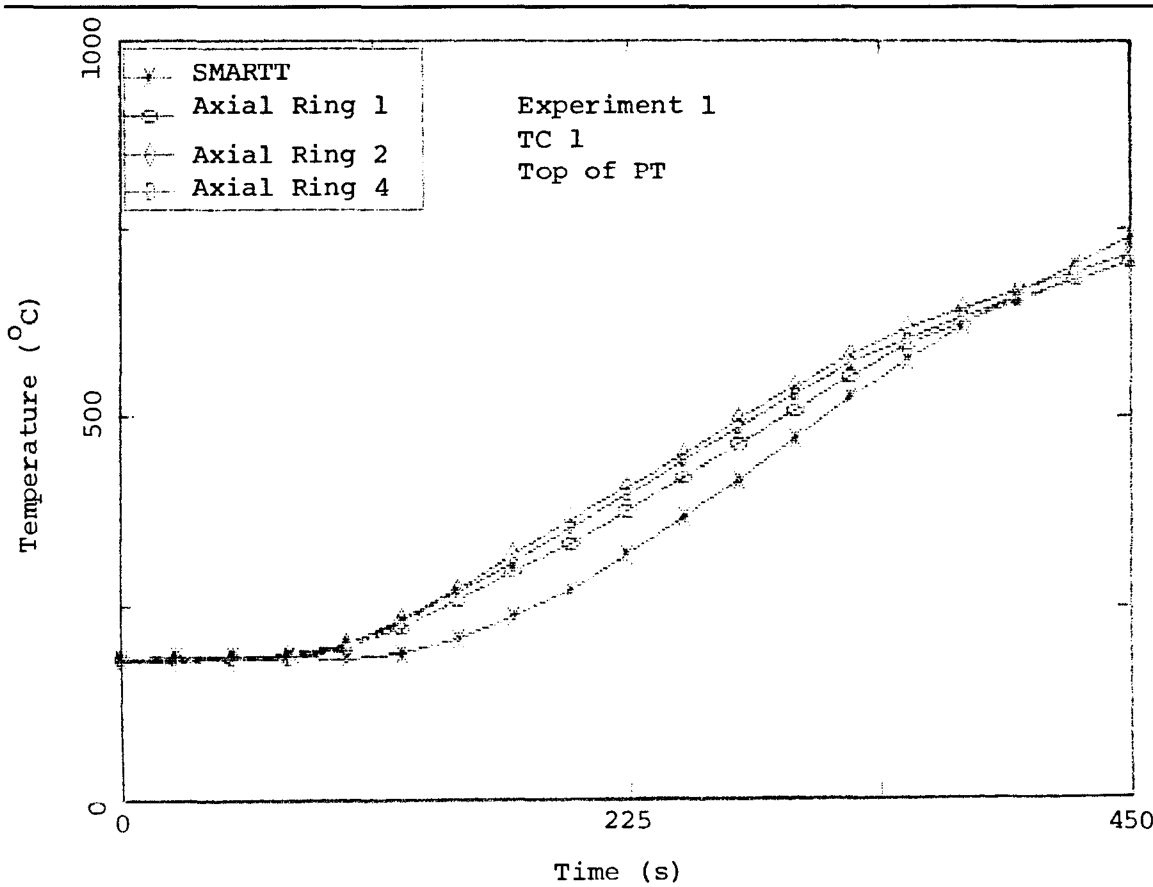

Figure 13: Comparison of measured and predicted PT temperatures in test 1.

information be released without the written consent of the COG–CANDEV Program Manager.

The experiments described in this paper were performed at Atomic Energy of Canada Limited's Whiteshell Nuclear Research Establishment. The experiments were performed by G.E. Gillespie, C.B. So, and R.G. Moyer.

References

1. *Locke KE, Archinoff GH, Muzumdar AP.* SMARTT – A computer code to predict fuel and pressure tube circumferential temperature gradients under asymmetric coolant conditions. Proc of 6th Annual CNS Conference, Ottawa, June 1985.
2. *Lowe PD, Archinoff GH, Luxat JC, Locke KE, Muzumdar AP.* Comparison of pressure tube delta-T experimental results with SMARTT code predictions. Proc 12th Annual Symposium on Simulation of Reactor Dynamics and Plant Control, Hamilton, Ontario, April 22–23 1986.
3. *Hussein E, Luxat JC.* Fuel cooling under channel steam venting conditions. Proc of 6th Annual CNS Conference, Ottawa, June 1985.